Available online at www.derpharmachemica.com

Scholars Research Library

Der Pharma Chemica, 2015, 7(10):23-33
(http://derpharmachemica.com/archive.html)

ISSN 0975-413X
CODEN (USA): PCHHAX

Experimental and theoretical study on the corrosion inhibition of mild steel by ethyl 1-(((4-acetylphenyl)((3-(ethoxycarbonyl)-1H-pyrazol-1-yl)methyl)amino) methyl)-5-methyl-1H-pyrazole-3-carboxylate in sulfuric acid solution

S. EL Arouji[1], K. Alaoui Ismaili[1], A. Zerrouki[2], S. El Kadiri[2], A. El Assyry[3], Z. Rais[1], M. Filali Baba[1], M. Taleb[1], A. Zarrouk[2], A. Aouniti[2] and B. Hammouti[2]

[1]Laboratoire d'Ingénierie d'Electrochimie de Modélisation et d'Environnement (LIEME) FSDM Fès, Morocco
[2]LCAE-URAC18, Faculty of Science, Mohammed first University, Oujda, Morocco
[3]Laboratoire d'Optoélectronique et de Physico-chimie des Matériaux (Unité associée au CNRST), Département de Physique, Université Ibn Tofail, Kénitra, Morocco

---

ABSTRACT

The corrosion inhibition of mild steel in 0.5 M H_2SO_4 using ethyl 1-(((4-acetylphenyl)((3-(ethoxycarbonyl)-1H-pyrazol-1-yl)methyl)amino)methyl)-5-methyl-1H-pyrazole-3-carboxylate (APC) at 298 K have been investigated. The study was performed using weight loss method, potentiodynamic polarization, and electrochemical impedance spectroscopy (EIS). The experimental results suggest that the inhibition efficiency of this compound increases with the increase in inhibitor concentration. Adsorption of this compound on mild steel surface obeys Langmuir's isotherm. Polarization measurements proved that this inhibitor behave as mixed type. EIS data showed that the charge transfer resistance of mild steel increases in acid solution containing inhibitor. Correlation between quantum chemical calculations and inhibition efficiency of the investigated compound is discussed using the Density Functional Theory method (DFT).

Keywords: Mild steel, EIS, Polarization, Weight loss, DFT, Acid inhibition

---

INTRODUCTION

Organic and inorganic compounds are widely used as corrosion inhibitors to control the corrosion [1-13]. Corrosion inhibition of mild steel is a matter of theoretical as well as practical importance [14]. Mild Steel is an extensively used metal in the industries, especially for structural applications, but it has high rate of dissolution in acidic medium, which is a major obstacle in its use on a large scale. Acids are widely used in industries such as pickling, cleaning, and descaling. Since the acids are highly aggressive, inhibitors are used to reduce the rate of dissolution of metals [15-19]. Use of corrosion inhibitors is one of the best methods to control the corrosion in acidic medium. Corrosion process in metals can be controlled by treating them in solutions of special compounds which would be able to interact with the metal and thus their surface gets modified. For this type of surface modification the most efficient inhibitors are organic compounds with a molecular structure of π-conjugation.

The efficiency of an organic compound, to act as a corrosion inhibitor, depends on its ability to adsorb and interact with metal atoms through their heteroatom. Compounds containing nitrogen, sulphur, and oxygen have been reported as inhibitors [20-26]. The basic action of inhibitor is attributed to an increase in ohmic resistance of an inhibitor film at the electrolyte interface or due to some type of adsorption on the metal surface. Adsorption of inhibitor on the metal-solution interface is accompanied by a change in potential difference between the metal electrode and the solution due to the non-uniform distribution of electric charges at the interface.

The prime aim of this paper is to evaluate the inhibition effectiveness of the inhibitor ethyl 1-(((4-acetylphenyl)((3-(ethoxycarbonyl)-1H-pyrazol-1-yl)methyl)amino)methyl)-5-methyl-1H-pyrazole-3-carboxylate (APC) on the mild steel corrosion in 0.5 M H_2SO_4 solution and attempt to study the interaction mechanism between the inhibitor molecule and the mild steel surface. Specifically, the inhibition properties of APC for mild steel in 0.5 M H_2SO_4 solution have been investigated using various methods, including weight loss, potentiodynamic polarization and electrochemical impedance spectroscopy (EIS). Meanwhile, quantum chemical calculations have been used to optimize the structure of APC and calculate the quantum chemical parameters of molecular related to its function as corrosion inhibitor. The molecular structure of APC is given in Figure 1.

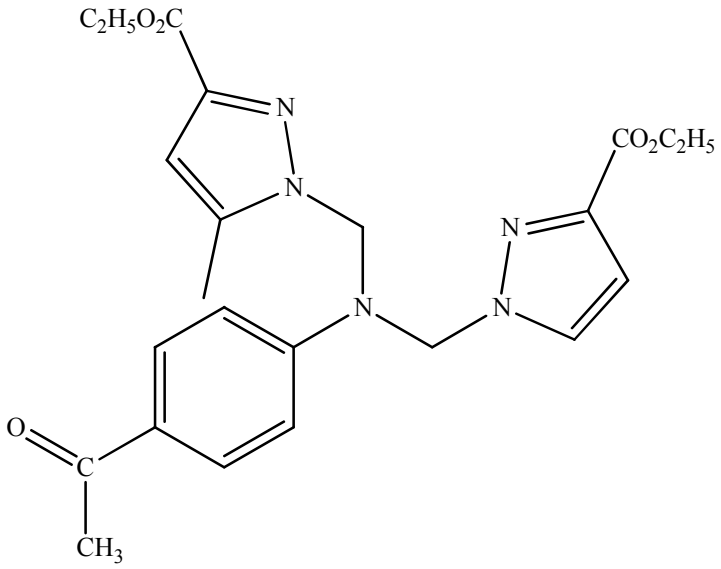

Figure 1: Molecular structure of APC

MATERIALS AND METHODS

Materials

The steel used in this study is a mild steel with a chemical composition (in wt%) of 0.09%P, 0.01 % Al, 0.38 % Si, 0.05 % Mn, 0.21 % C, 0.05 % S and the remainder iron (Fe). The steel samples were pre-treated prior to the experiments by grinding with amery paper sic (220, 400, 800, 1000 and 1200); rinsed with distilled water, degreased in acetone, washed again with bidistilled water and then dried at room temperature before use.

Solutions

The aggressive solutions of 0.5 M H_2SO_4 were prepared by dilution of analytical grade 98% H_2SO_4 with distilled water. The concentration range of ethyl 1-(((4-acetylphenyl)((3-(ethoxycarbonyl)-1H-pyrazol-1-yl)methyl) amino) methyl)-5-methyl-1H-pyrazole-3-carboxylate (APC) used was 10^{-6}M to 10^{-3}M.

Gravimetric study

Gravimetric experiments were performed according to the standard methods [27], the mild steel sheets of 2 × 1 × 0.2 cm were abraded with a series of emery papers SiC (120, 600 and 1200) and then washed with distilled water and acetone. After weighing accurately, the specimens were immersed in a 50 mL beaker containing 100 mL of 0.5 M H_2SO_4 solution with and without addition of different concentrations inhibitor. All the aggressive acid solutions were open to air. After 6 h of acid immersion, the specimens were taken out, washed, dried, and weighed accurately. In order to get good reproducibility, all measurements were performed few times and average values were reported to obtain good reproducibility. The inhibition efficiency (η_{WL}%) and surface coverage (θ) were calculated as follows:

$$C_R = \frac{W_b - W_a}{At} \quad (1)$$

$$\eta_{WL}(\%) = \left(1 - \frac{w_i}{w_0}\right) \times 100 \quad (2)$$

$$\theta = \left(1 - \frac{w_i}{w_0}\right) \quad (3)$$

where W_b and W_a are the specimen weight before and after immersion in the tested solution, w_0 and w_i are the values of corrosion weight losses of mild steel in uninhibited and inhibited solutions, respectively, A the total area of the mild steel specimen (cm^2) and t is the exposure time (h).

Electrochemical measurements

The electrochemical measurements were carried out using Volta lab (Tacussel- Radiometer PGZ 100) potentiostate and controlled by Tacussel corrosion analysis software model (Voltamaster 4) at under static condition. The corrosion cell used had three electrodes. The reference electrode was a saturated calomel electrode (SCE). A platinum electrode was used as auxiliary electrode of surface area of 1 cm^2. The working electrode was mild steel of the surface 1 cm^2. All potentials given in this study were referred to this reference electrode. The working electrode was immersed in test solution for 30 min to a establish steady state open circuit potential (E_{ocp}). After measuring the E_{ocp}, the electrochemical measurements were performed. All electrochemical tests have been performed in aerated solutions at 298 K. The EIS experiments were conducted in the frequency range with high limit of 100 kHz and different low limit 0.1 Hz at open circuit potential, with 10 points per decade, at the rest potential, after 60 min of acid immersion, by applying 10 mV ac voltage peak-to-peak. Nyquist plots were made from these experiments. The best semicircle can be fit through the data points in the Nyquist plot using a non-linear least square fit so as to give the intersections with the *x*-axis.

The inhibition efficiency of the inhibitor was calculated from the charge transfer resistance values using the following equation:

$$\eta_z\% = \frac{R_{ct}^{i} - R_{ct}^{\circ}}{R_{ct}^{i}} \times 100 \quad (4)$$

Where, R°_{ct} and R^{i}_{ct} are the charge transfer resistance in absence and in presence of inhibitor, respectively.

After ac impedance test, the potentiodynamic polarization measurements of mild steel substrate in inhibited and uninhibited solution were scanned from cathodic to the anodic direction, with a scan rate of 1 mV s^{-1}. The potentiodynamic data were analysed using the polarization VoltaMaster 4 software. The linear Tafel segments of anodic and cathodic curves were extrapolated to corrosion potential to obtain corrosion current densities (I_{corr}).
The inhibition efficiency was evaluated from the measured I_{corr} values using the following relationship:

$$\eta_{Tafel}(\%) = \frac{I_{corr} - I_{corr(i)}}{I_{corr}} \times 100 \quad (5)$$

where I_{corr} and $I_{corr(i)}$ are the corrosion current densities for steel electrode in the uninhibited and inhibited solutions, respectively.

Quantum chemical calculations

Complete geometrical optimizations of the investigated molecules are performed using DFT (density functional theory) with the Beck's three parameter exchange functional along with the Lee-Yang-Parr nonlocal correlation functional (B3LYP) [28-30] with 6-31G* basis set is implemented in Gaussian 03 program package [31]. This approach is shown to yield favorable geometries for a wide variety of systems. This basis set gives good geometry optimizations. The geometry structure was optimized under no constraint. The following quantum chemical parameters were calculated from the obtained optimized structure: The highest occupied molecular orbital (E_{HOMO}) and the lowest unoccupied molecular orbital (E_{LUMO}), the energy difference (ΔE) between E_{HOMO} and E_{LUMO}, dipole moment (μ), electron affinity (A), ionization potential (I) and the fraction of electrons transferred (ΔN).

RESULTS AND DISCUSSION

Potentiodynamic polarization curves

The polarization behavior of mild steel in acid solutions without and with different concentrations of APC are shown in Figure 2 of the supporting information. The electrochemical parameters such as I_{corr}, E_{corr}, and Tafel slopes (β_c)

were calculated by extrapolating the Tafel lines to the corresponding corrosion potential, and they are listed in Table 1. From Figure 2 of the Supporting Information, it is clear that both anodic (dissolution of metal) and cathodic (hydrogen evolution) reactions were retarded after the introduction of inhibitor to the acid media. The inhibition of corrosion enhanced with an increase in inhibitor concentration. In the presence of different APC concentrations, the E_{corr} of mild steel shifted around ±16.3 mV as compared to the blank in H_2SO_4. Inhibitors are said to be cathodic or anodic, only if the E_{corr} values are displaced more than ±85 mV as compared to the blank [32]. This indicates that APC inhibited the corrosion of mild steel in mixed mode. The cathodic domain curves appeared as parallel lines indicating that the introduction of APC to the acidic media did not alter the hydrogen evolution mechanism, and the reduction of H^+ ions at the surface of metal takes place mainly through a charge transfer mechanism [33,34].

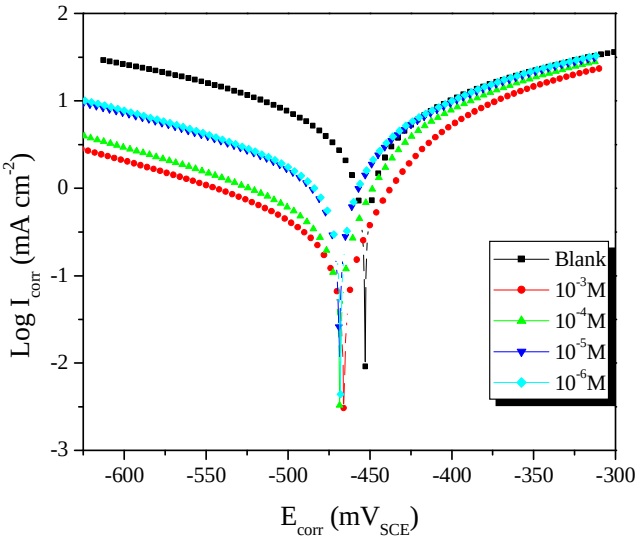

Figure 2: Tafel plots of APC on mild steel in 0.5 M H_2SO_4

Table 1: Electrochemical kinetic parameters obtained by Tafel polarization technique for mild steel in absence and presence of various concentrations APC at 298 K

Medium	Conc (M)	$-E_{corr}$ (mV/SCE)	$-\beta_c$ (mV dec^{-1})	I_{corr} (μA cm^{-2})	η_{Tafel} (%)
H_2SO_4	0.5	452.9	232.5	6861.6	—
APC	10^{-3}	466.4	184.8	1735.0	75
	10^{-4}	467.8	128.4	2329.2	66
	10^{-5}	469.2	213.9	2976.1	56
	10^{-6}	466.3	230.9	3550.7	48

From table 1 The increase in inhibition efficiency with increasing inhibitor concentration may be attributed to the formation of a barrier film, which prevents the attack of acid on the metal surface [35]. The best inhibition efficiency was about 75% at concentration 10^{-3} M.

EIS

Fig. 3 shows the Nyquist plots of mild steel in 0.5 M H_2SO_4 in uninhibited and inhibited solutions containing various concentrations of APC. The Nyquist plots reveal that each impedance diagram consists of a large capacitive loop at high frequencies (HF) and an inductive loop at low frequencies (LF) both in the absence and presence of inhibitor. The presence of two time constants for iron dissolution at Ecorr in the absence of inhibitors has been reported in the literature [36]. The HF capacitive loop could be attributed to the double layer capacity in parallel with the charge transfer resistance (R_{ct}). The LF inductive loop may be originated from the relaxation process obtained by adsorption species as H^+_{ads} and SO_4^{2-} on the surface of the metal [37]. It may also be attributed to the re-dissolution of the passivated surface at low frequencies [38]. Fig. 3 reveals that increase in concentration of APC results in increase in size of the semicircle, which is an indication of the inhibition of the corrosion process. It is observed that capacitive semicircles in the absence and presence of APC were depressed with centre under the real axis. This is attributed to the dispersion effect and the state of the electrode surface [39].

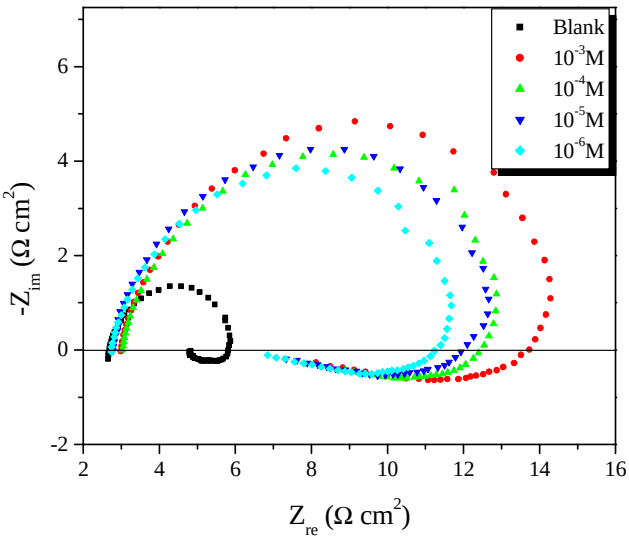

Figure 3: Nyquist plots for mild steel recorded in 0.5 M H_2SO_4 in the absence and presence of different concentrations of APC at 298 K

Table 2: Impedance parameters with corresponding inhibition efficiency for the corrosion of mild steel in 0.5 M H_2SO_4 at different concentrations of APC

Medium	Conc (M)	R_{ct} (Ω cm^2)	C_{dl} (μF cm^{-2})	η_z (%)
H_2SO_4	0.5	2.8	229.8	—
APC	10^{-3}	9.2	109.0	70
	10^{-4}	8.4	151.6	67
	10^{-5}	8.2	155.7	66
	10^{-6}	7.3	173.3	62

The values of the electrochemical parameters derived from Nyquist plots are given in Table 2. It can be observed that the values of R_{ct} increase while the values of C_{dl} decrease with increase in concentration of APC. The decrease in C_{dl} on the introduction of APC to the acid solution indicates the presence of a protective layer that covers the surface of the electrode. The adsorption of APC on the mild steel surface decreases C_{dl} because they displaced the water molecules and other ions that were originally adsorbed on the surface. With higher concentration of APC, either the thickness of the protective layer or the surface coverage by APC increased due to more APC electrostatically adsorbed on the electrode surface [40].

Gravimetric studies

The values of corrosion rate in the absence and presence of various concentrations of APC at different 298 K are given in Table 3. The fractional surface coverage θ can be easily determined from the weight loss measurements by the ratio $\eta_{WL}(\%)/100$, where $\eta_{WL}(\%)$ is inhibition efficiency and calculated using relation 2. The data obtained suggest that the APC get adsorbed on the mild steel surface at studied temperature and corrosion rates increased in absence and presence of inhibitor in 0.5 M H_2SO_4 solutions. Table 3 indicates that the corrosion rate of mild steel decreased on increasing concentration. This behavior could be attributed to the increase in adsorption of APC at the metal/solution interface on increasing its concentration. Indeed, the adsorption of the APC could occur due to the formation of links between the d-orbital of iron atoms, involving the displacement of water molecules from the metal surface, and the lone sp2 electron pairs present on the N and/or O atoms [41]. The order of the inhibition efficiency from the weight loss measurements are in good agreement with those obtained from the EIS and potentiodynamic polarization methods.

Table 3: Effect of APC concentration on corrosion data of steel in 0.5 M H_2SO_4

Medium	Conc (M)	C_R (mg/cm^2 h)	θ	η_{WL} (%)
Blank	1.0	1.608	—	—
APC	10^{-3}	0.102	0.75	75
	10^{-4}	0.547	0.66	66
	10^{-5}	0.579	0.64	64
	10^{-6}	0.611	0.62	62

Adsorption isotherm and thermodynamic parameters

The adsorption on the corroding surfaces never reaches the real equilibrium and tends to reach an adsorption steady state. However, when the corrosion rate is sufficiently small, the adsorption steady state has a tendency to become a quasi-equilibrium state. In this case, it is reasonable to consider the quasi-equilibrium adsorption in thermodynamic way using the appropriate equilibrium isotherms [42]. The efficiency of this compound as a successful corrosion inhibitor mainly depends on its adsorption ability on the metal surface. So, it is essential to know the mode of adsorption and the adsorption isotherm that can give valuable information on the interaction of inhibitor and metal surface. The surface coverage values, θ (η_{WL}(%)/100) for different concentrations of APC was used to explain the best adsorption isotherm. A plot of C/θ versus C (Fig. 4) gives a straight line with an average correlation coefficient of 0.99957 and a slope of nearly unity suggests that the adsorption of APC molecules obeys Langmuir adsorption isotherm, which can be expressed by the following equation:

$$\frac{C}{\theta} = \frac{1}{K} + C \qquad (6)$$

where C is inhibitor concentration and K is the equilibrium constant for the adsorption-desorption process.

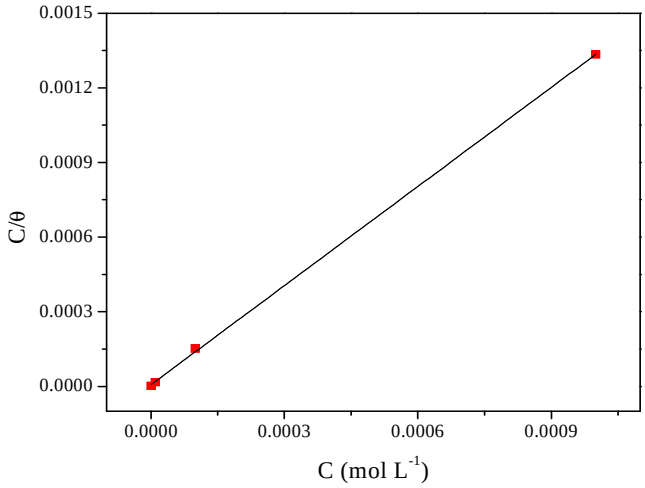

Figure 4: Langmuir adsorption isotherm of APC on the steel surface

The thermodynamic parameters from the Langmuir adsorption isotherm are listed in Table 4, together with the value of the Gibbs free energy of adsorption ΔG°_{ads} calculated from the equation:

$$\Delta G^{\circ}_{ads} = -RTLn(55.5K) \qquad (7)$$

Where R is the universal gas constant, T the thermodynamic temperature and the value of 55.5 is the concentration of water in the solution [43].

The value K calculated from the reciprocal of intercept of isotherm line as 148337.36 L mol^{-1}. The high value of the adsorption equilibrium constant reflects the high adsorption ability of this inhibitor on mild steel surface.

Table 4: Thermodynamic parameters for the adsorption of APC in 0.5 M H_2SO_4 on the mild steel at 298K

Inhibitor	K_{ads} (M^{-1})	R^2	ΔG°_{ads} (KJ/mol)
APC	148337.36	0.99957	-39.45

From Eq. (7), the ΔG°_{ads} was calculated as -39.45 kJ mol^{-1}. The negative value of standard free energy of adsorption indicates spontaneous adsorption of APC molecules on mild steel surface and also the strong interaction between inhibitor molecules and the metal surface[44,45]. Generally, the standard free energy values of -20 kJ mol^{-1} or less negative are associated with an electrostatic interaction between charged molecules and charged metal surface (physical adsorption); those of -40 kJ mol^{-1} or more negative involves charge sharing or transfer from the inhibitor molecules to the metal surface to form a co-ordinate covalent bond (chemical adsorption) [46,47]. The value of ΔG°_{ads} in our measurement is -39.45 kJ mol^{-1} (in Table 4), it is suggested that the adsorption of this APC derivative involves two types of interaction, chemisorption and physisorption [48].

Quantum chemical calculation results

To investigate the effect of molecular structure on the inhibition mechanism and inhibition efficiency, some quantum chemical calculations were performed. Quantum chemical parameters such as the energy of highest occupied molecular orbital (E_{HOMO}), the energy of the lowest unoccupied molecular orbital (E_{LUMO}), HOMO-LUMO energy gap (ΔE_{gap}), the dipole moment (μ) of optimized molecular and structures of the inhibitor APC (Fig. 5) had been calculated (Table 5). Frontier molecular orbital theory suggests that the formation of a transition state is due to an interaction between frontier orbitals (HOMO and LUMO) of reacting species. It is well-known that low absolute values of the energy band gap gives good inhibition efficiencies, because the ionization potential will be low [49]. The dipole moment (μ) is a measure of the polarity of a covalent bond, which is related to the distribution of electrons in a molecule [50]. Although literature is inconsistent with the use of μ as a predictor for the direction of a corrosion inhibition reaction, it is generally agreed that the large values of μ favor the adsorption of inhibitor [51]. As it is shown in Table 5, the APC has a low ΔE_{gap} (3.755 eV), which implies the high ability to accept electrons from the d-orbital of Fe and a high stability of the [Fe-APC] complexes [52]. Moreover, APC has a rather high value of μ (4.2759 D), which implies the strong adsorption of molecule at the mild steel surface.

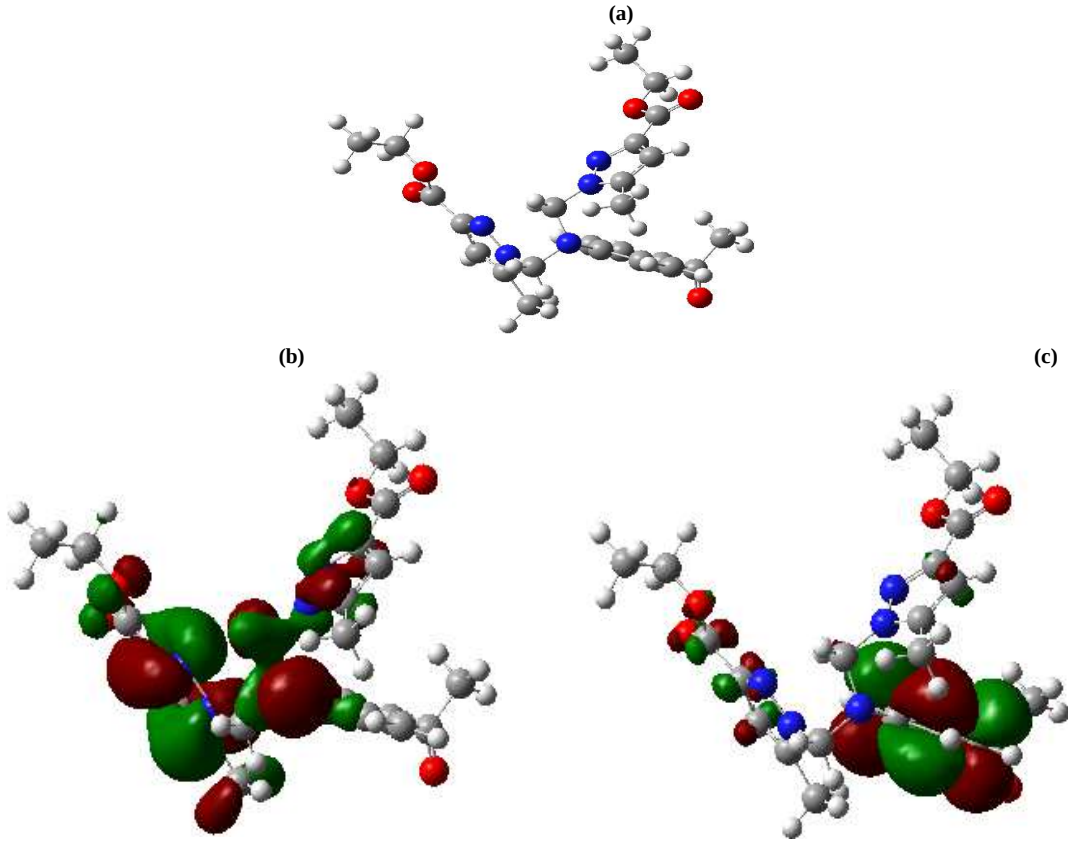

Figure 5: Optimized molecular structure of APC (a), HOMO (b), LUMO (c) orbitals

Another method to correlate inhibition efficiency with parameters of molecular structure is to calculate the fraction of electrons transferred from inhibitor to metal surface. According to Koopman's theorem [53], E_{HOMO} and E_{LUMO} of the inhibitor molecule are related to the ionization potential (I) and the electron affinity (A), respectively. The ionization potential (I) and the electron affinity (A) are defined as follows:

$I = -E_{HOMO}$ (8)

$A = -E_{LUMO}$ (9)

Then absolute electronegativity (χ) and global hardness (η) of the inhibitor molecule are approximated as follows [54]:

$$\chi = \frac{I + A}{2} \quad (10)$$

$$\eta = \frac{I - A}{2} \quad (11)$$

Thus the fraction of electrons transferred from the inhibitor to metallic surface, ΔN, is given by [55]:

$$\Delta N = \frac{\chi_{Fe} - \chi_{inh}}{2(\eta_{Fe} + \eta_{inh})} \quad (12)$$

To calculate the fraction of electrons transferred the theoretical values of of χ_{Fe} (7 eV mol^{-1}) and of η_{Fe} (0 eV mol^{-1}) are used [56]. The calculated results are presented in Table 5.

Table 5: Calculated quantum chemical parameters of the studied compound

Quantum parameters	APC
E_{HOMO} (eV)	-8.707
E_{LUMO} (eV)	-4.952
ΔE gap (eV)	3.755
μ (debye)	4.2759
$I = -E_{HOMO}$	8.707
$A = -E_{LUMO}$	4.952
$\chi = \frac{I + A}{2}$	6.8295
$\eta = \frac{I - A}{2}$	1.8775
$\Delta N = \frac{\chi_{Fe} - \chi_{inh}}{2(\eta_{Fe} + \eta_{inh})}$	0.04541

Generally, value of ΔN shows inhibition efficiency resulting from electron donation, and the inhibition efficiency increases with the increase in electron-donating ability to the metal surface. Value of ΔN show inhibition effect resulted from electrons donation. According to Lukovits's study [57], if ΔN < 3.6, the inhibition efficiency increases with increasing electron-donating ability at the metal surface.

Mechanism of inhibition

Generally, corrosion inhibition mechanism in acid medium is the adsorption of inhibitor onto the metal surface. As far as the inhibition process is concerned, it is generally assumed that adsorption of the inhibitor at the metal/solution interface is the first step in the action mechanism of the inhibitors in aggressive acid media. Four types of adsorption may take place during inhibition involving organic molecules at the metal/solution inter-face: (1) electrostatic attraction between charged molecules and the charged metal, (2) interaction of unshared electron pairs in the molecule with the metal, (3) interaction of π-electrons with the metal, and (4) a combination of the above [58]. Concerning inhibitors, the inhibition efficiency depends on several factors; such as the number of adsorption sites

and their charge density, molecular size, heat of hydrogenation, mode of interaction with the metal surface, and the formation metallic complexes [59]. Physical adsorption requires presence of both electrically charged surface of the metal and charged species in the bulk of the solution; the presence of a metal having vacant low-energy electron orbital and of an inhibitor with molecules having relatively loosely bound electrons or heteroatom with lone pair electrons. However, the compound reported can be protonated in an acid medium. Thus they become cations, existing in equilibrium with the corresponding molecular form:

$$APC + xH^+ \leftrightarrow \left[APC_x\right]^{x+} \quad (13)$$

The protonated APC, however, could be attached to the mild steel surface by means of electrostatic interaction between SO_4^{2-} and protonated APC since the mild steel surface has positive charge in the H_2SO_4 medium [60]. This could further be explained based on the assumption that in the presence of SO_4^{2-}, the negatively charged SO_4^{2-} would attach to positively charged surface and thereby protonated APC being adsorbed to the metal surface. Apart from electrostatic interaction, some chemical interaction is also involved. The non-bonding electrons of hetero atoms and π-electrons of aromatic ring caused chemical interaction.

CONCLUSION

The inhibition effect of ethyl 1-(((4-acetylphenyl)((3-(ethoxycarbonyl)-1H-pyrazol-1-yl)methyl)amino)methyl)-5-methyl-1H-pyrazole-3-carboxylate (APC) on the corrosion of mild steel in 0.5 M H_2SO_4 was studied using chemical and electrochemical techniques. APC has a good inhibition effect for corrosion of mild steel in acidic solutions to form a protective film, and it absorbs on the metal surface according to Langmuir adsorption isotherm. The inhibition efficiency increases with increasing inhibitor concentration. The polarization curves 0.5 M H_2SO_4 indicate that APC behaves as mixed type inhibitor by inhibiting both anodic metal dissolution and cathodic hydrogen evolution reaction. The ΔG_{ads}° value suggest that this interaction may occur in both physical and chemical adsorption. All the results obtained from EIS, polarization and weight loss are in good agreement. Through the quantum chemical calculations, we have shown that the calculated parameters are correlated with the experimental results, and it was found that inhibition effect increased with the lower ΔE_{gap} and the higher μ values.

REFERENCES

[1] O.K. Abiola, J.O.E. Otaigbe, O.J. Kio, Gossipium hirsutum, *Corros. Sci.* **2009**, 51, 1879.
[2] D. Mercier, M.-G. Barthés-Labrousse, *Corros. Sci.* **2009**, 51, 339.
[3] K.C. Emeregul, A.A. Aksut, *Corros. Sci.* **2000**, 42, 2051.
[4] A.H. Al Hamzi, H. Zarrok, A. Zarrouk, R. Salghi, B. Hammouti, S.S. Al-Deyab, M. Bouachrine, A. Amine, F. Guenoun, *Int. J. Electrochem*. Sci., **2013**, 8, 2586.
[5] A. Zarrouk**,** B. Hammouti, H. Zarrok, I. Warad, M. Bouachrine, *Der Pharm. Chem*., **2011**, 3, 263.
[6] D. Ben Hmamou, R. Salghi, A. Zarrouk, M. Messali, H. Zarrok, M. Errami, B. Hammouti, Lh. Bazzi , A. Chakir, *Der Pharm. Chem*., **2012**, 4, 1496.
[7] A. Ghazoui, N. Bencaht, S.S. Al-Deyab, A. Zarrouk, B. Hammouti, M. Ramdani, M. Guenbour, *Int. J. Electrochem. Sci*., **2013**, 8, 2272.
[8] A. Zarrouk, H. Zarrok, R. Salghi, N. Bouroumane, B. Hammouti, S.S. Al-Deyab, R. Touzani, *Int. J. Electrochem. S*ci., **2012**, 7, 10215.
[9] H. Bendaha, A. Zarrouk, A. Aouniti, B. Hammouti, S. El Kadiri, R. Salghi, R. Touzani, *Phys. Chem. N*ews, **2012**, 64, 95.
[10] S. Rekkab, H. Zarrok, R. Salghi, A. Zarrouk**,** Lh. Bazzi, B. Hammouti, Z. Kabouche, R. Touzani, M. Zougagh, *J. Mater. Environ. Sci*., **2012**, 3, 613.
[11] A. Zarrouk, B. Hammouti, H. Zarrok, M. Bouachrine, K.F. Khaled, S.S. Al-Deyab, *Int. J. Electrochem. Sci*., **2012**, 6, 89.
[12] A. Ghazoui, R. Saddik, N. Benchat, M. Guenbour, B. Hammouti, S.S. Al-Deyab, A. Zarrouk, *Int. J. Electrochem. Sci*., **2012**, 7, 7080.
[13] H. Zarrok, K. Al Mamari, A. Zarrouk, R. Salghi, B. Hammouti, S. S. Al-Deyab, E. M. Essassi, F. Bentiss, H. Oudda, *Int. J. Electrochem. Sci*., **2012**, 7, 10338.
[14] S.A. Ali, M.T. Saeed, S.V. Rahman, *Corros. Sci.* **2003**, 45, 253.
[15] H. Zarrok, A. Zarrouk, R. Salghi, Y. Ramli, B. Hammouti, M. Assouag, E. M. Essassi, H. Oudda and M. Taleb, *J. Chem. Pharm. Res*., **2012**, 4, 5048.
[16] A. Zarrouk, B. Hammouti, A. Dafali, F. Bentiss, *Ind. Eng. Chem. Res.* **2013**, 52, 2560.

[17] H. Zarrok, A. Zarrouk, R. Salghi, H. Oudda, B. Hammouti, M. Assouag, M. Taleb, M. Ebn Touhami, M. Bouachrine, S. Boukhris, *J. Chem. Pharm. Res*. **2012**, 4, 5056.
[18] H. Zarrok, H. Oudda, A. El Midaoui, A. Zarrouk, B. Hammouti, M. Ebn Touhami, A. Attayibat, S. Radi, R. Touzani, *Res. Chem. Intermed*. **2012**, 38, 2051.
[19] A. Ghazoui, A. Zarrouk, N. Bencaht, R. Salghi, M. Assouag, M. El Hezzat, A. Guenbour, B. Hammouti, *J. Chem. Pharm. Res*. **2014**, 6, 704.
[20] H. Zarrok, A. Zarrouk, R. Salghi, M. Ebn Touhami, H. Oudda, B. Hammouti, R. Touir, F. Bentiss, S.S. Al-Deyab, *Int. J. Electrochem. Sci*. **2013**, 8, 6014.
[21] A. Zarrouk, H. Zarrok, R. Salghi, R. Touir, B. Hammouti, N. Benchat, L.L. Afrine, H. Hannache, M. El Hezzat, M. Bouachrine, *J. Chem. Pharm. Res*. **2013**, 5, 1482.
[22] H. Zarrok, A. Zarrouk, R. Salghi, M. Assouag, B. Hammouti, H. Oudda, S. Boukhris, S.S. Al Deyab, I. Warad, *Der Pharm. Lett*. **2013**, 5, 43.
[23] D. Ben Hmamou, M.R. Aouad, R. Salghi, A. Zarrouk, M. Assouag, O. Benali, M. Messali , H. Zarrok, B. Hammouti, *J. Chem. Pharm. Res*. **2012**, 4, 3498.
[24] M. Belayachi, H. Serrar, H. Zarrok, A. El Assyry, A. Zarrouk, H. Oudda, S. Boukhris, B. Hammouti, Eno E. Ebenso, A. Geunbour, *Int. J. Electrochem. Sci*. **2015**, 10, 3010.
[25] H. Tayebi, H. Bourazmi, B. Himmi, A. El Assyry, Y. Ramli, A. Zarrouk, A. Geunbour, B. Hammouti, Eno E.Ebenso, *Der Pharm. Lett*. **2014**, 6(6), 20.
[26] H. Tayebi, H. Bourazmi, B. Himmi, A. El Assyry, Y. Ramli, A. Zarrouk, A. Geunbour, B. Hammouti, *Der Pharm. Chem*. **2014**, 6(5), 220.
[27] ASTM, G 31-72, American Society for Testing and Materials, Philadelphia, PA, **1990**.
[28] A. D. Becke, *J. Chem. Phy*. **1992**, 96, 9489.
[29] A. D. Becke, *J. Chem. Phy*. **1993**, 98, 1372.
[30] C. Lee, W. Yang, R.G. Parr, *Phy. Rev. B* **1988**, 37, 785.
[31] M.J. Frisch, G.W. Trucks, H.B. Schlegel, G.E. Scuseria, M.A. Robb, J.R. Cheeseman, J.A. Montgomery Jr., T. Vreven, K.N. Kudin, J.C. Burant, J.M. Millam, S.S. Iyengar, J. Tomasi, V. Barone, B. Mennucci, M. Cossi, G. Scalmani, N. Rega, G.A. Petersson, H. Nakatsuji, M. Hada, M. Ehara, K. Toyota, R. Fukuda, J. Hasegawa, M. Ishida, T. Nakajima, Y. Honda, O. Kitao, H. Nakai, M. Klene, X. Li, J.E. Knox, H.P. Hratchian, J.B. Cross, C. Adamo, J. Jaramillo, R. Gomperts, R.E. Stratmann, O. Yazyev, A.J. Austin, R. Cammi, C. 870 H. Ju et al. / Corrosion Science 50 (2008) 865-871 Pomelli, J.W. Ochterski, P.Y. Ayala, K. Morokuma, G.A. Voth, P. Salvador, J.J. Dannenberg, V.G. Zakrzewski, S. Dapprich, A.D. Daniels, M.C. Strain, O. Farkas, D.K. Malick, A.D. Rabuck, K. Raghavachari, J.B. Foresman, J.V. Ortiz, Q. Cui, A.G. Baboul, S. Clifford, J. Cioslowski, B.B. Stefanov, G. Liu, A. Liashenko, P. Piskorz, I. Komaromi, R.L. Martin, D.J. Fox, T. Keith, M.A. Al- Laham, C.Y. Peng, A. Nanayakkara, M. Challacombe, P.M.W. Gill, B. Johnson, W. Chen, M.W. Wong, C. Gonzalez, J.A. Pople, Gaussian 03, Revision C.02, Gaussian Inc., Pittsburgh, PA, **2003**.
[32] A.K. Satapathy, G. Gunasekaran, S.C. Sahoo, K. Amit, P.V. Rodrigues, *Corros. Sci*. **2009**, 51, 2848.
[33] R. Solmaz, G. Kardas, M.C. Ulha, B. Yazici, M. Erbil, *Electrochim. Acta* **2008**, 53, 5941.
[34] M. Elayyachy, A. Idrissi, B. Hammouti, *Corros. Sci*. **2006**, 48, 2470.
[35] O. Benali, M. Ouazene, *Arab. J. Chem.* **2011**, 4, 443.
[36] S.A. Umoren, Y. Li, F.H. Wang, *Corros. Sci*. **2010**, 52, 2422.
[37] P.C. Okafor, Y. Zheng, *Corros. Sci*. **2009**, 51, 850.
[38] E.M. Sherif, S.-M. Park, *Electrochim. Acta* **2006**, 51, 1313.
[39] K.F. Khaled, K. Babic´-Samardz˘ija, N. Hackerman, *Corros. Sci*. **2006**, 48, 3014.
[40] J. Zhao, G. Chen, *Electrochim. Acta* **2012**, 69, 247.
[41] H. Zarrok, A. Zarrouk, B. Hammouti, R. Salghi, C. Jama, F. Bentiss, *Corros. Sci*. **2012**, 64, 243.
[42] L.J. Vracar, D.M. Drazic, *Corros. Sci*. **2002**, 44, 1669.
[43] O. Olivares, N. V. Likhanova, B. Gomez, J. Navarrete, M.E. Llanos-Serrano, E. Arce, J. M. Hallen, *Appl. Surf. Sci*. **2006**, 252, 2894.
[44] G. Avci, *Mater. Chem. Phys*. **2008**, 112, 234.
[45] E. Bayol, A.A. Gurten, M. Dursun, K. Kayakırılmaz, *Acta Phys. Chim. Sin*. **2008**, 24, 2236.
[46] O.K. Abiola, N.C. Oforka, *Mater. Chem. Phys*. **2004**, 83, 315.
[47] M. Ozcan, R. Solmaz, G. Kardas, I. Dehri, *Colloid Surf. A* **2008**, 325, 57.
[48] S. Zhang, Z. Tao, W. Li, B. Hou, *Appl. Surf. Sci*. **2009**, 255, 6757.
[49] Gokhan Gece, *Corros. Sci*. **2008**, 50, 2981.
[50] El Sayed H. El Ashry, Ahmed El Nemr, Sami A. Esawy, Safaa Ragab, *Electrochim. Acta* **2006**, 51, 3957.
[51] N.O. Eddy, B.I. Ita, *J. Mol. Model*. **2011**, 17, 359.
[52] E.E. Oguzie, C.K. Enenebeaku, C.O. Akalezi, S.C. Okoro, A.A. Ayuk, E.N. Ejike, *J. Colloid Interface Sci*. **2010**, 349, 283.
[53] M. Lebrini, M. Lagrenee, M. Traisnel, L. Gengembre, H. Vezin, F. Bentiss, *Appl. Surf. Sci*. **2007**, 253, 9267.
[54] V.S. Sastri, J.R. Perumareddi, *Corrosion* **1997**, 53, 671.

[55] R.G. Pearson, *Inorg. Chem*. **1988**, 27, 734.
[56] S. Martinez, *Mater. Chem. Phys*. **2002**, 77, 97.
[57] I. Lukovits, E. Kalman, F. Zucchi, *Corrosion* **2001**, 57, 3.
[58] H. M. Bhajiwala, R. T. Vashi, *Bull. Electrochem*. **2001**, 17, 441.
[59] D. Schweinsberg, G. George, A. Nanayakkara, D. Steinert, *Corros. Sci*. **1988**, 28, 33.
[60] A. Fouda, M. Moussa, F. I. Taha, A. I. ElNeanaa, *Corros. Sci*. **1986**, 26, 719.